# Profiling the neoplasm microenvironment of silica nanomaterial-derived scaffolds of single, 2- and 3-composite systems

Victor Akpe[1, 2*], Shweta Murhekar[1, 2], Tak H. Kim[1, 2], Christopher L. Brown[1, 2] and Ian E. Cock[1, 2*]

[1] Environmental Futures Research Institute, Griffith University, Nathan Campus, QLD 4111, Australia.

[2] School of Environment and Science, Griffith University, Nathan Campus, QLD 4111, Australia.

*Correspondence: I.Cock@griffith.edu.au

**ORCID** : VA, (0000-0001-8639-321X); THK, (0000-00024495-176X); CLB, (0000-0001-5135-0244); IEC, (0000-0002-8732-8513)

## Abstract

The challenges with scaffold profiling of cell-based assay includes accelerated cancer cell proliferation, induced scaffold toxicity, and identifying irrelevant cancer cell-based assays in batch assessments. The current work investigates profiling carcinoma of breast cancer cells of MCF-7 model systems using silica nanoparticles (SNP) scaffold sourced from synthetic materials and plant extracts. Herein, the engineered tissue scaffolds were used to create temporary structures for cancer cell attachments, differentiation, and subsequently to assess the metabolic activity of the cancer cell colonies. The cell viability of the cancer cells was assessed using the tetrazolium compound (MTS reagent), which was reduced to coloured formazan, to indicate metabolically active cancer cells in a proliferating assay. We aimed to develop cancer cell-based scaffolds that not only mimic the neoplastic activity, but that also allowed synergistic interaction with cisplatin for *in vitro* assay screening.

Keywords: Silica nanoparticles, nanomaterial scaffolds, probit analysis , cancer cell metabolic activity, cisplatin, MCF-7 cells

## 1.Introduction

Despite human cancer-derived cell lines having long been successfully used in the laboratories, methods for cell-based assay screening have continuously been questioned with regards to their biological relevance. Alternative traditional culture models for drug screening are of considerable interest in biological and synthetic model systems that can mimic the neoplasm environment. [1-3] The clinical efficacy of drug candidates in some of the tumour models have remained a subject of debate

over the past decades. Clearly, the metastasis process remains the main cause of death of cancer patients, [4] and understanding the tumour microenvironment may lead to improved drug strategies.

Many drug candidates designed from the traditional (standard) cell lines model for carcinomas such as breast cancer, pancreatic, colorectal, prostate do not show clinical efficacy as, [1, 4] (1) some models lack key physiological features for tumour environment; (2) cell-based assay have been traditionally performed on immortalized cell lines, with large genetic drifts over time in cell growth, [5] (3) large concentration of fetal serum and nutrients facilitate rapid growth, which promotes rapid differentiation and cell functions, [6] (4) planar rigidity on some cancer cell lines grown on 2-dimensional cell culture substrates may limit the rapid deformation of cells; required to mimic the *in* vivo environment. Another important technical challenge in cell-based scaffold screening is identifying irrelevant cell-based assays since the neoplastic environment is complex and is *terra incognita*.

The healthy normal cells react to stimuli primarily through trans-membrane proteins - the integral part of the extracellular matrix (ECM) system. [7, 8] These proteins regulate biochemical and biomechanical functions including, morphology, cell differentiation and growth, gene expression, and cellular responses to drugs, etc. [7] For example, extracted tissue from animals containing collagen, laminin, and elastin have been used as ECM-tissue scaffolds for organoid [9, 10] and tumoroid [11] applications. A drawback with the use of ECM-relevant tissue culture environment is the batch variation in constitutions, placing limitations to the implementation of *in vitro* cell culture environments.

Another setback with the standard culture growth is the homeostasis imbalance during periodic nutrient replacements. [8] It has been argued that for cancer cells to spread there must be interactions with homeostatic factors responsible for tumor growth, survival, invasion, and metastasis. [12, 13] Some studies have suggested that cancer cells do not interact exclusively but with co-culture cells in their microenvironments. [14, 15] Stephen Paget's hypothesis (1889) had previously described cancer mechanism as the crosstalk between selected cancer cells (seed) and the microenvironment (soil).[16] A retrospect of Paget's hypothesis extensively discussed by Fidler IJ et al. [12, 17, 18] may suggest the reason some cancer cells grown on standard culture flasks and subsequently used as drug screening platforms have not been suitable models for drug screening.

Apart from the planar constraints imposed on some cancer cell lines grown on 2-dimensional cell culture substrates, cells are often confined to mimic the *in vitro*, 2-dimensional state, and not the *in vivo* environment. While the standard culture method remains the acceptable, scientific standard for cultivating and reviving cell culture cell lines, investigating the dynamic changes over time, observing cancer cells differentiation and landscape changes, may require alternative 2- or 3 -dimensional amendable scaffold support systems.

This work investigates a new building approach for scaffold construct based on the bottom-up assembly, derived from a single, 2- and 3-composite matrix systems of SNP. The objective of our study was to understand if the scaffold compositions could induce growth differentiation, and to profile the synergistic interaction with cisplatin for *in vitro* assay screening.

# 2. Materials and methods

The tissue culture flasks (25 $cm^2$, Corning) were supplied by Invitrogen, Australia. Abcam, Australia supplied the green, fluorescent dye, cytopainter (ab176735) used for imaging cells. Cisplatin was purchased from Tocris Bioscience (Minneapolis, USA) and supplied by Invitrogen, Australia.

The following reagents supplied by Sigma-Aldrich, Australia include, Ludox AS-40 colloidal silica nanoparticles (SNP), polyethylene glycol, (PEG-8000) and polyamidoamine first generation ($1^o$ PAMAM) dendrimer. Thermofisher Scientific, Australia, supplied the cell culture reagents, Dulbecco's Modified Eagle Medium (DMEM), penicillin-streptomycin, fetal bovine serum (FBS), TrypLE™ Express Enzyme (1X) with no phenol red and Hanks balanced salt solution (HBSS). The scanning electron microscopy (SEM) was used to acquire the initial crystal-like lattices formed from the nanocomposite casts. For the SEM preparations, the samples were mounted on aluminum stubs using adhesive carbon coated in 2.5 nm platinum with a Leica EM ACE600 platinum coater, or 10 nm carbon using a Safematic carbon coater. All samples were imaged at 5 kV using the In-beam secondary electron detector on a Tescan MIRA3 field emission SEM. The SNP size was (Ø , 20-30 nm) was determined by dynamic light scattering (DLS) method from a previous study. [19] A customized rectangular box made of polyvinyl chloride (PVC) was used for the fabrication of the silica derived scaffold. The rectangular PVC box consist of Peltier heaters, heating pads, RadioShack consisting of 12V DC Micro Fan and two humidity-temperature monitors specifications. The silica derived scaffolds were fabricated under the following conditions, Δ= 37°C, 15% humidity and 30°C, 90% humidity, with ±3 humidity and temperature fluctuations, prior to seeding of cancer cells . Just before the scaffolds were constructed, water was filled to the lower tray designated for the high humidity chamber. The upper trays in both chambers were perforated to create effective convective airflow.

## 2.1 Scaffold formation

The stock solution (40 wt. %) of SNP was diluted with sterile deionised water across the range 40.0 to 1 wt. %. Similar preparation was carried out for PEG-8000. Stoichiometric ratios of the 2-composite mixture (SNP and PEG) were from 40: 1, respectively. The 3-composite mixture was obtained by mixing the 2-composite mixture with a branched $1^o$ PAMAM dendrimer in the respective ratios specified in the figures. The preparation of the composite mixture is in a separate supplementary file. The 2-

composite (SNP and PEG) mixture was stirred at room temperature for 4 hours for even dispersion. The 3-composite mixture was stirred for 24 hours at 4°C. A 100 µL volume of the mixtures was transferred to 96 well plates under low and high humidity conditions, according to the following specifications: Δ= 37°C, 15% humidity and 30°C, 90% humidity.

NT Wild Harvest, Australia supplied the *Terminalia ferdinandiana* Exell. (commonly known as Kakadu plum) fruit and leaf material used in the mixture for the SNP derived scaffolds. The materials dried to achieve a constant mass followed by prolonged drying time according to previously reported protocol. [20] Briefly, Kakadu plum leaves and fruit were separately dried in Sunbeam dehydrator and ground into powders. The individual 1 g masses of powdered fruit and leaves were weighed into separate tubes and extracted using 50 mL of a) methanol b) deionized water c) ethyl acetate d) hexane or e) chloroform. The tubes were placed on a shaker for 24hrs at 4°C. Subsequently, individual extract was filtered using Whatman 54 filter paper under vacuum to remove particulate matter, with the extracts dried at 50°C under the same vacuum. The extract residue obtained in solid was dissolved in 10 mL of deionised water containing 1% dimethyl sulfoxide (DMSO). ThermoFischer, Australia supplied the 0.22µm syringe filter used to filter particulates greater than the diameter specifications before the extracts were finally collected at 4°C. The 3-composite mixture was obtained by mixing previously obtained 40.0-1.0 (wt. %) PEGylated SNP (SNP: PEG) fractions with either fruit or leaf extracts for 24hrs at 4°C. A 100 µL volume of the mixtures was transferred to 96 well plates (supplied by Sarstedt in Australia) under low and high humidity conditions, according to the following specifications: Δ= 37°C, 15% humidity and 30°C, 90% humidity.

## 2.4 Cell culture preparation

MCF-7 breast cancer cell line was obtained from the American Type Culture Collection (ATCC) and used as the cancer model for this study. The cancer cells were cultured aseptically in a laminar flow biological safety cabinet class II and maintained in DMEM media. The culture media was supplemented with 5 % FBS and penicillin/streptomycin (0.1% of the working culture medium). All cell culture processes were performed in a humified incubator at 5% $CO_2$, 37 °C. Once 80% confluence had been achieved, TryLE™ Express was added to the culture flasks to detach the adherent cells, followed by the addition of further culture media (twice the initial volume of TryLE™ Express) to prevent membrane damage through prolonged exposure to trypsin. The detached cells were centrifuged at 2500 rpm for 5 min, the supernatant was discarded and they were obtained as pellets. The cells were then washed in Hanks balanced salt solution (HBSS) and into 1 mL of fresh cell culture media, calculated at a concentration of $10^3$ cells$ml^{-1}$.

## 2.5 Cancer cell viability study

Promega, Australia supplied the MTS kit used for the viability assay. A volume of 100 µL ($10^3$ cells.ml$^{-1}$) of seeded cells were transferred on the nanocomposite substrate casts and incubated at 24 and 48 hrs in 4 x 96-well micro-test plates (Sarstedt). Before the transfer, each plate was cast with either: 1. SNP, 2. PEGylated SNP, 3. PEGylated SNP with polyamido amine first generation (1$^o$ PANAM dendrimer), 4. *T. ferdinandiana* fruit extracts were mixed with PEGylated SNP, and 5. *T. ferdinandiana* fruit extracts were mixed with PEGylated SNP. Subsequently, 20 µL of Promega solution was added to each well and the plates incubated for 1 hour. The absorbances at 490 nm was recorded using a Molecular Devices, Spectra Max M3 plate reader. All tests were performed in at least duplicate and duplicate controls were included on each plate. We maintained sterile substrate casts throughout the cell culture experiment.

The cell proliferation of the bioassay is expressed by, $\varphi = \frac{\sum_{i=1}^{n}(\mu-\bar{s})_{c,t}}{\sum_{i=1}^{n}(\bar{y}-\bar{\emptyset})_t}$ **(1)**

With the standardisation correction, the cell viability is expressed by:

$$\varphi = (k^*)\frac{\sum_{i=1}^{n}(\mu-\bar{s})_{c,t}}{\sum_{i=1}^{n}(\bar{y}-\bar{\emptyset})_t} \times 100 \quad \textbf{(2)}$$

$\sum_{i=1}^{n} x(c,t)$, are the concentration-time dependent cellular response variables upon exposure to the nanocomposite substrate (s); n is the number of samples, and $x_s$, is the cellular response on the substrate cast; $\mu$, is the average cellular response; $\bar{s}$, is the mean response from the substrate cast without cells; $y\,(t)$, is the cellular response without the substrate cast. $\bar{y}$, is the mean cellular response without the substrate cast, and $\bar{\emptyset}$, is the mean data from the empty well plate (blank). $k^*$, is the outlier correction factor, which is 0.5.

## 2.6 Fluorescent imaging

A volume of 200 µL ($10^3$ cells/mL) of MCF-7 cells was seeded into each well on the 24-well plate, previously cast with SNP derived nanocomposite substrate casts. The plates were then incubated for either 24 or 48 hours at 37$^o$C, 5% $CO_2$. The attached cells were stained with green, fluorescent cytopainter dye (ab 176735) according to the Abcam protocol. After 24 hrs, the cells had reached 80 % confluence. These were washed with fresh media and 200 µL of green cytopainter solution was added and incubated for 2 hrs in the cell culture chamber. The cells were then washed with 200 µL of HBSS buffer solution. The staining protocol was repeated for a parallel cell culture after 48 hrs of incubation for comparison.

## 2.7 Chemosensitivity of MCF-7 cells to cisplatin/ SNP derived scaffolds

A volume of 100 µL of cell culture containing $10^3$ cells/mL was added to individual wells of a 96-well control plate. When the cells attained 80% confluency, 20 µL of cisplatin was added to each well at the following concentrations: 7.5, 15, 22.5, 30, 37.5 and 45 µg/mL, and incubated for 24 hrs at 37 $^oC$ using 5% $CO_2$ in the culture chamber. A volume of 20 µL of MTS solution was added to each well and the plates incubated for another 1 hour. The absorbance was measured at 490 nm on a plate reader. The same procedure was repeated with the following substrate casts: 1. PEGylated SNP; 2. PEGylated SNP mixed with KPLM; and 3. PEGylated SNP mixed with KPFE. All tests were performed in at least duplicate and duplicate controls were included on each plate. Sterile conditions of the substrate casts were obtained by exposing the plates to UV radiation for at least 30 minutes before the cell culture experiment.

## 2.8 Statistical analyses

The probit transformation data for the cell viability at 24- and 48 hrs, along with the computational analysis from the Microsoft program Excel (2016) software package, were used to analyse statistically relevant data; gauged by $0 < p < 0.06$ or 94% confidence interval limit. This confidence interval limit makes allowance for batch variations that are inevitable in cell-based scaffold assays. The batch effect in this study is the microstructural changes on substrate cast over time as a result of exposure to temperature changes. This effect was adjusted by filtering the non-biological response from the direct absorbance reading of substrate and blank and standardising the cell viability data. The error bars on the charts are represented as relative standard deviation of 5% (n=4).

# Results and discussion

This present work investigates the profiling of scaffold construct utilizing bottom-up assembly of composite matrix systems derived from SNP. We aimed from our study to understand: (1) if the scaffold compositions could induce growth differentiation; and (2) profile breast cancer cells of MCF-7 exposed to cisplatin dose. The preliminary design focused on the preparation of a single, 2- and 3-composite substrates derived from SNP using the bottom-up approach. [21] The main advantage of assembling a solid composite material from extended basic building structures, is the rearrangement of the particles using van der Waals and other short-range intermolecular forces, packing to the minimum energy crystal-like configuration lattices. This arrangement depends on the surface condition, temperature, humidity, convectional airflow, and on the precursor materials. [22, 23] The convectional airflow creates the mass transfer of the solutes to spread away from the center while the heating causes a capillary flow within the evaporating mixture by the Marangoni flow process. [24,

[25] Consequently, as the solvent evaporates, different surface patterns are formed (Figure 1). Nanocomposite platform derived from a bottom-up approach offers simplicity and may allow molecular interactions from unlikely neighboring particles via a non-covalent bonding interaction.

In Figure 1, SNP was used as the precursor, synthetic material to build a robust environment for cancer cell models utilized in this study. The biomimicry tendencies of SNP have been reported in some biomedical applications. [26-28] Some of these properties include size (5-1000 nm), biocompatibility, non-covalent interactions that improves spatial topology, chemical inertness, and low toxicity. The controlled pore-size of assembled SNP has also been reported as an efficient drug delivery cargo, [29] including adsorption of protein and release. [30] Thus, using the self-assembly approach, we were able to build multiple coordination within the same nanoparticles. PEG inclusion in SNP mixture is known to increase the bioavailability for drug uptake [31] and in our previous study, [32] PEG was used as a cosolvent to increase interactions with unlikely molecules. The PAMAM dendrimers are polymeric nanoparticles formed by repetitive units of dendrite-like compound. These molecules have the tendency to form a highly monodispersed polymer in solution. [33, 34] The surface chemistry is particularly intriguing as PAMAM dendrimers are driven by electrostatic and hydrophobic interactions. [34] In this study, inclusion of PAMAM dendrimer was used to create a 3-composite scaffold. Furthermore, fabrication of scaffolds at low and high humidity conditions was used to increase the variance in the "soil" environment for cancer cells differentiation.

Thus, breast cancer cells of MCF-7 cells were exposed to synthetic scaffold composites of SNP, SNP: PEG, and SNP : PEG : PAMAM dendrimer using scaffold developed under low and high humidity conditions. The cell viability of the cancer cells was assessed using the tetrazolium compound (MTS reagent), which changed by reducing to coloured formazan, to indicate metabolically active cancer cells in a proliferating assay. Figure 2 shows the viability of cancer cells exposed to the different composite materials. Whilst the first 24 hrs of cancer exposure to scaffolds increased the metabolic activity in Figure 2: charts 1a,1b, there were slow metabolic activities of MCF-7 cells in charts 2a, 2b, 3a and 3b. Further, exposure of MCF-7 cells to the different scaffold composites at 48 hrs reduced the metabolic activities, except for Figure 2: chart 3a, which suggest increased metabolic activities. Since the variance in metabolic activities were more significant in some scaffold assays than others, we used a benchmark of 50% cell viability after 48 hrs to differentiate viable assay count from non-viable assay counts, indicated in Figure 2.

The same procedure was used for the scaffold composite containing plant extraction from *T. ferdinandiana* leaf methanolic (KPLM) and Kakadu plum fruit, ethyl acetate (KPFE) extracts in Figure 3. The charts in Figure 3 : charts 4 and 5 using the 50% cell viability benchmark suggests no viable count assays after 48 hrs. *T. ferdinandiana* is a rich source of ascorbic acid and is known for its

antioxidant activity. It acts as a substrate for the redox enzyme ascorbate, which the plants use for stress resistance. Also, the presence of ascorbate prevents free radical formation. The plant primarily uses the stored ascorbic acid to remove oxygen. The phytochemical studies of *T. ferdinandiana* from a previous study [35] indicates a diversity of tannins in both the fruit and leaf extracts. Notably, tannins in some selected human cancer cells inhibited proliferation. [36] Since the extraction does not preclude the crude mixture, we presume that the extraction also contains other unidentified phytochemical compounds. The inclusion of plant in the scaffold development was to understand if this would change the cancer cells differentiation.

A confidence interval limit with a statistical *p*-value of 0.06 was used to suggest statistically relevant data. Notably, the *p*-value (0.06) as opposed to 0.05 was used to make allowance for batch variations that are inevitable in cell-based scaffold assays. Thus, the assay profiling in Table 1, for MCF-7 cells viability, indicate SNP : PEG and SNP: PEG: KPFE as promising cancer-cell candidates for a 48-hr evaluation for this study. Additionally, the inhibitory concentration ($IC_{50}$) plot was used to assess the toxicity assessment of MCF-7 cells exposed to the different composite scaffold assays. These are indicated in Figures 4 and 5, from figure plots of 1 to 5, respectively. Table 2 shows the calculated inhibitory concentration of the scaffolds required to reduce the cell viability of MCF-7 cells by 50 %.

Additionally, the fluorescent images of MCF-7 cells exposed to SNP derived composite scaffolds were used to assess MCF-7 cells growth pattern within the first 24 hrs. Some general concepts into tumour biology [37] have indicated that : (i) the tumor metabolism is initiated by stress; (ii) hypoxia is present in tumour microenvironment and exerts a corresponding effect on cancer metabolism; (iii) tumour cells have metabolic activities; and differ from quiescence cell cycle states (the cells that do not replicate until they are activated); and (iv) induced change in metabolic enzymes may affect tumorigenesis. Most studies have also shown that the tumor cells differ from normal cells, are biologically heterogeneous, contain multiple subtype phenotypes with different invasive and metastasis processes. These carcinomas exhibit variable cell size with no defined shape, uninhibited cell replication and proliferation, and some tumour cells have been known to resist treatments. [38] In addition, the tumor microenvironment may be subject to dynamic and environmental changes over time.

In Figures 6 and 7, the fluorescent images of MCF-7 cells were stained with the green cytopainter, according to the procedure described in the methods section. Cytopainter mainly binds to the cytoplasm of a living cell. In Figure 6, diagrams (a) show clustered cells in micrograph 2, with the other micrographs in a quiescence state. This suggests that the cancer cells did not replicate in the SNP:PEG scaffolds in the first 24 hrs and the cell viability after 48 hrs indicate a reduction. The quiescence state of cancer cells was also observed for the 3-composite scaffolds from SNP: PEG: dendrimer in Figure 6,

diagram (b). The 3-composite scaffold assays that consisted of SNP: PEG: KPFE on the other hand, induced cancer cell cluster formation for the first 24 hrs.

The cisplatin dosing (25 µM to 150 µM) were exposed to MCF-7 for 24 hrs and used as the control plate. Figure 8a. shows the cancer cell viability for the control. Since the cell viability for cancer cells are not significantly different in the control plate, we used the cumulative distribution plot. Subsequently, this plot was used to calculate the combined cisplatin dosing/scaffold concentration for inhibiting MCF-7 cells by at least 50 %. Figures 8b to 8d correspond to the plots for the assigned cisplatin dosing exposed to scaffold assays. Table 3 shows that it only required 2.5 µM of cisplatin exposure to inhibit cancer cells grown on SNP:PEG composite scaffold as opposed to other scaffolds that required higher cisplatin dosing.

# 4. Conclusion

One of the characteristics of a tumour environment is that the metabolic activities can be measured by conventionally calculating the cell viability. However, the calculation becomes cumbersome when cancer cells are grown on scaffold-based model systems. Some of the challenges with scaffold profiling of a cancer cell-based assay includes among other factors, accelerated cancer cell proliferation, induced scaffold toxicity, and identifying irrelevant cancer cell-based assays in batch assessments.
This study investigated the cell viability of MCF-7 cells exposed to different composite scaffolds at 24- and 48-hr intervals. The goal was to develop cancer cell-based scaffolds that not only can mimic the neoplastic activity, but with synergistic interaction with cisplatin for *in vitro* assay screening.

Firstly, we identified viable and non-viable count assays using 50% cell viability benchmark along with the calculation of the *p*-value. Based on this study, there were more inhibitory cancer cell-based model systems accounted for than proliferating assays (viable count assays). SNP:PEG and SNP:PEG:KPFE scaffold composites have both 0 viable assay count and *p*-value was significantly lower than 0.06. Since the goal of our investigation was not to proliferate the cancer cells rapidly, a reduction of cancer cell viability by 20-30% after 48 hrs incubation was considered suitable before use as *in vitro* scaffolds for drug screening.

Additionally, the fluorescent images of the different composite scaffolds suggest that by varying the constitution of the scaffolds, the cancer cells environment can be fine-tuned. Here, we identified the tendency of the MCF-7 cells to form cluster cells with composite scaffold containing SNP: PEG: KPFE, whereas SNP: PEG and SNP:PEG: dendrimer remained mostly in the quiescence state within the first 24 hrs. Also, the shape of the cluster cells and their formation suggest the scaffold environment is tractable to an extent. The different scaffolds and control exposed to MCF-7 cells suggest SNP:PEG

as the system that requires the minimum dosing concentration (2.5 μM) to reduce the cell viability by at least 50%.

This study demonstrates the alternative method for using scaffold-based model systems synergistically with anticancer drug to profile an *in vitro* neoplasm environment. The scaffold composites are amenable, with the prospect of using this building block to establish a three-dimensional neoplasm environment.

## Supplementary material

Supplementary Figure S1
Supplementary Figure S2
Supplementary Figure S3
Supplementary Figure S4
Supplementary Figure S5
Supplementary Figure S6
Supplementary Figure S7
Supplementary Table S1
Supplementary Table S2
Supplementary Table S3
Supplementary Table S4

# References


1. Horvath P, Aulner N, Bickle M, Davies AM, Del Nery E, Ebner D, Montoya MC, Östling P, Pietiäinen V, Price LS : Screening out irrelevant cell-based models of disease. *Nature Reviews Drug discovery* 2016; **15**, 751-769.
2. Edmondson R, Broglie JJ, Adcock AF, Yang L: Three-dimensional cell culture systems and their applications in drug discovery and cell-based biosensors. *Assay and Drug Development Technologies* 2014; **12**, 207-218.
3. Gillet J-P, Varma S, Gottesman MM: The clinical relevance of cancer cell lines. *Journal of the National Cancer Institute* 2013; **105**, 452-458.
4. Eckhardt BL, Francis PA, Parker BS, Anderson RL: Strategies for the discovery and development of therapies for metastatic breast cancer. *Nature Reviews Drug Discovery* 2012; **11**, 479-497.
5. Verjans E-T, Doijen J, Luyten W, B. Landuyt, Schoofs L: Three-dimensional cell culture models for anticancer drug screening: worth the effort? *Journal of Cellular Physiology* 2018; **233**, 2993-3003.
6. Redshaw Z, Loughna P T: Oxygen concentration modulates the differentiation of muscle stem cells toward myogenic and adipogenic fates. *Differentiation* 2012; **84**, 193-202.
7. Cavo M, Fato M, Peñuela L, Beltrame F, Raiteri R, Scaglione S: Microenvironment complexity and matrix stiffness regulate breast cancer cell activity in a 3D in vitro model. *Scientific Reports* 2016; **6**, 35367
8. Abbott A, Cyranoski D: biology's new dimension. *Nature* 2003;**424**, 870-872.
9. Fatehullah A, Tan SH, Barker N: Organoids as an in vitro model of human development and disease. *Nature Cell Biology* 2016; **18**, 246-254.
10. Gjorevski N, Sachs N, Manfrin A, Giger S, Bragina ME, Ordóñez-Morán P, Clevers H, Lutolf MP: Designer matrices for intestinal stem cell and organoid culture. *ON Nature* 2016; **539**,560-564.

11. Ji K, Sameni M, Osuala K, Moin K, Mattingly RR, Sloane BF: Spatio-temporal modeling and live-cell imaging of proteolysis in the 4D microenvironment of breast cancer. *Cancer and Metastasis Reviews*. 2019; **38**, 445-454.
12. Fidler IJ : The pathogenesis of cancer metastasis: the 'seed and soil' hypothesis revisited. *Nature Reviews. Cancer* 2003; **3**, 453-458.
13. Witz IP, Levy-Nissenbaum O: The tumor microenvironment in the post-PAGET era. *Cancer Letters* 2006; **242**, 1-10.
14. Huang Z, Zhang M, Chen G, Wang W, Zhang P, Yue Y, Guan Z, Wang X, Fan J: Bladder cancer cells interact with vascular endothelial cells triggering EGFR signals to promote tumor progression. *International Journal of Oncology* 2019; **54**, 1555-1566.
15. Haridas P, Penington CJ, McGovern JA, McElwain DS, Simpson MJ: Quantifying rates of cell migration and cell proliferation in co-culture barrier assays reveals how skin and melanoma cells interact during melanoma spreading and invasion. *Journal of Theoretical Biology* 2017; **423**, 13-25.
16. Fidler IJ: The pathogenesis of cancer metastasis: the'seed and soil'hypothesis revisited. *Nature Reviews Cancer* 2003; **3**, 453-458.
17. Fidler IJ: Selection of successive tumour lines for metastasis. *Nature New Biology* 1973; **242**, 148-149.
18. Fidler IJ, Hart IR: Biological diversity in metastatic neoplasms: origins and implications. *Science* 1982; **217**, 998-1003.
19. Akpe V: Controlled, self-assembly of silica nanoparticles into uniform mesostructured glass. *Master's Thesis, University of Sydney*, NSW 2006, Australia 2017.
20. Shalom J, Cock IE: Fruit and leaf extracts inhibit proliferation and induce apoptosis in selected human cancer cell lines. *Nutrition and Cancer* 2018;**70**, 579-593.
21. Fu J, Gu Z, Liu Y, Zhang J, Song H, Yang Y, Yang Y, Noonan O, Tang J, Yu C: Bottom-up self-assembly of heterotrimeric nanoparticles and their secondary Janus generations. *Chemical Science* 2019; **10**, 10388-10394.
22. Canning J, Ma M, Gibson BC, Shi J, Cook K, Crossley MJ: Highly ordered mesoporous silica microfibres produced by evaporative self-assembly and fracturing. *Optical Materials Express* 2013; **3**, 2028-2036.
23. Naqshbandi M, Canning J, Gibson BC, Nash MM, Crossley MJ: Room temperature self-assembly of mixed nanoparticles into photonic structures. *Nature Communications* 2012; **3**, 1-7.
24. Majumder M, Rendall CS, Eukel JA, Wang JY, Behabtu N, Pint CL, Liu T-Y, Orbaek AW, Mirri F, Nam J: Overcoming the “coffee-stain” effect by compositional Marangoni-flow-assisted drop-drying. *The Journal of Physical Chemistry B* 2012; **116**, 6536-6542.
25. Nikolov AD, Wasan DT, Chengara A, Koczo K, Policello GA, Kolossvary I: Superspreading driven by Marangoni flow. *Advances in Colloid and Interface Science* 2002; **96**, 325-338.
26. Zhao F, Wang X, Ding B, Lin J, Hu J, Si Y, Yu J, Sun G: Nanoparticle decorated fibrous silica membranes exhibiting biomimetic superhydrophobicity and highly flexible properties.*RSC Advances* 2011; **1**, 1482-1488.
27. Jackson E, Ferrari M, Cuestas-Ayllon C, Fernández-Pacheco R, Perez-Carvajal J, de la Fuente JsM, Grazú V, Betancor L: Protein-templated biomimetic silica nanoparticles. *Langmuir* 2015; **31**, 3687-3695.
28. Chai S, Zhang J, Yang T, Yuan J, Cheng S: Thermoresponsive microgel decorated with silica nanoparticles in shell: Biomimetic synthesis and drug release application. *Colloids and Surfaces A: Physicochemical and Engineering Aspects* 2010;**356**, 32-39.
29. Argyo C, Weiss V, Bräuchle C, Bein T: Multifunctional mesoporous silica nanoparticles as a universal platform for drug delivery.*Chemistry of Materials* 2014; **26**, 435-451.

30. Saikia J, Yazdimamaghani M, Hadipour Moghaddam SP, Ghandehari H: Differential protein adsorption and cellular uptake of silica nanoparticles based on size and porosity. *ACS Applied Materials & Interfaces* 2016; **8**, 34820-34832.
31. Halas NJ: Nanoscience under glass: the versatile chemistry of silica nanostructures *ACS Nano* 2008; **2**, 179-183.
32. Akpe V, Shiddiky MJ, Kim TH, Brown CL, Yamauchi Y, Cock IE: Cancer biomarker profiling using nanozyme containing iron oxide loaded with gold particles *Journal of the Royal Society Interface* 2020; **17**, 20200180.
33. Maiti PK, Çağın T, Wang G, Goddard WA: Structure of PAMAM dendrimers: Generations 1 through 11. *Macromolecules* 2004; **37**, 6236-6254.
34. Wang B, Sun Y, Davis T P, Ke PC, Wu Y, Ding F: Understanding effects of pamam dendrimer size and surface chemistry on serum protein binding with discrete molecular dynamics simulations. *ACS Sustainable Chemistry & Engineering* 2018; **6**, 11704-11715.
35. Wright MH, Sirdaarta J, White A,. Greene AC, Cock IE: GC-MS headspace analysis of Terminalia ferdinandiana fruit and leaf extracts which inhibit Bacillus anthracis growth. *Pharmacognosy Journal* 2017; **9**,73-82.
36. Shalom J, Cock IE: Terminalia ferdinandiana Exell. fruit and leaf extracts inhibit proliferation and induce apoptosis in selected human cancer cell lines. *Nutrition and Cancer* 2018;**70**, 579-593.
37. Romero-Garcia S, Lopez-Gonzalez JS, B´ez-Viveros JL, Aguilar-Cazares D, Prado-Garcia H: Tumor cell metabolism: an integral view. *Cancer Biology & Therapy* 2011; **12**, 939-948.
38. Akpe V, Kim TH, Brown CL, Cock IE: Circulating tumour cells: a broad perspective. *Journal of The Royal Society Interface* 2020;**17**, 20200065.

# Acknowledgement

V.A acknowledges the Griffith University for the GUPR and GUIPR scholarships, and the research grant towards the doctoral programme.

# Legends and Figures

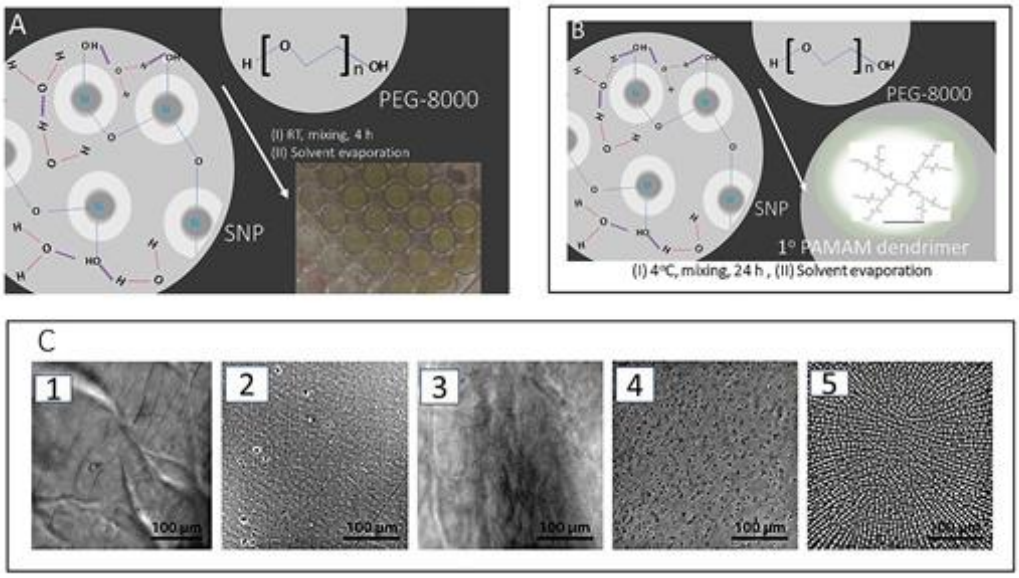


**Fig. 1.** Schematic of silica nanocomposite cast derived from single, 2-component and 3-component mixtures. A. Ludox colloidal silica (size, 20 nm) or SNP has the tendency to absorb water, and it is highly hydrophilic. This is indicated by the physical water absorption (red) and hydrogen bonding in purple, linked to silanol groups (Si-OH) and bridged to each other by an oxygen atom. The silica nanoparticles substrate cast was achieved in the 96-well plate at room temperature with a customised evaporation chamber. Subsequently, the same procedure was used to generate 2-composite substrate cast containing SNP: PEG-8000 in another well plate. B. Using the same method, a 3-composite substrate, containing SNP: PEG/1$^{o}$ PAMAM dendrimer and SNP:PEG/plant extracts were developed in a seperate 96-well plate. C. Optical images of the substrate cast surfaces (1) SNP (2) SNP: PEG (3) SNP: PEG mixed with 1$^{o}$ PAMAM dendrimer (4) SNP: PEG incorporated with *T. ferdinandiana* fruit ethyl acetate extract (KPFE) (5) SNP: PEG incorporated with *T. ferdinandiana* leaf methanolic extract (KPLM).

## 1. SNP scaffold assays

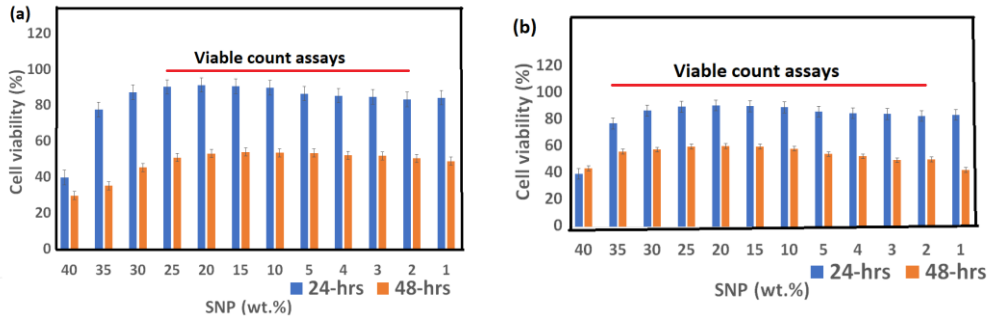


## 2. SNP:PEG composite scaffold assays

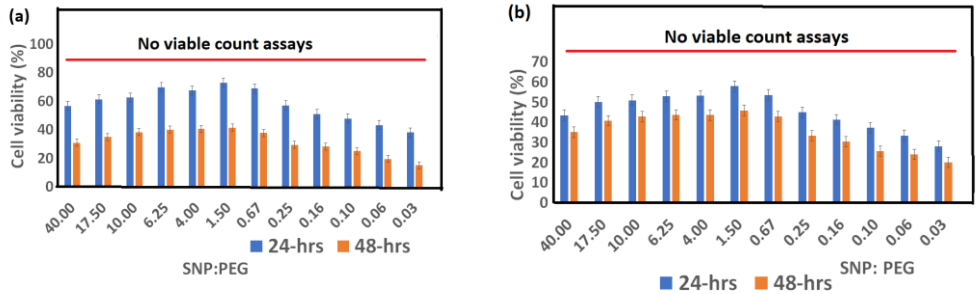


## 3. SNP : PEG : Dendrimer composite scaffold assays

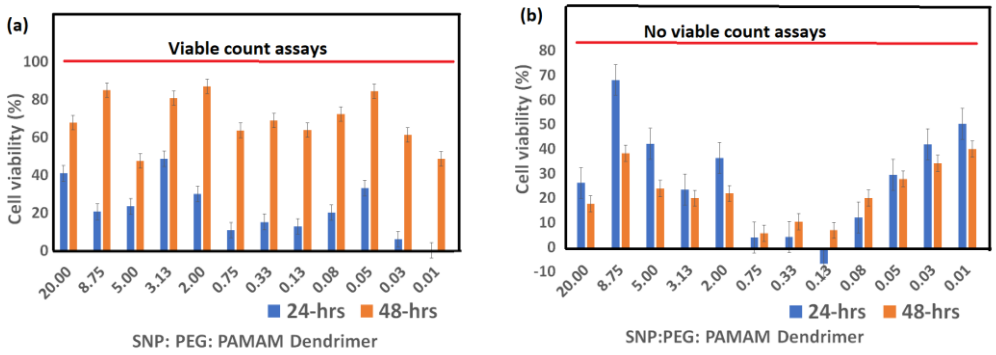


**Fig.2.** Cancer cell viability of SNP derived scaffolds from synthetic materials. Breast cancer cells of MCF-7 were exposed to synthetic derived materials. The substrate casts were developed under: (a) low humidity conditions (b) high humidity conditions as described in the methods section. The horizontal line above the bar charts indicate counting systems used to differentiate the viable count assays from the no viable count assays. Additionally, the data on the horizontal axis of chart 3, represent the concentration ratios that have been simplified (actual concentrations were used for the inhibitory concentrations figure plot 3 in Figure 4). The assay was considered viable when the viability of cancer cells was at least above 50%. Additionally, the 50% cell viability above benchmark were the cancer cells unaffected to scaffold exposure after 48 hrs. No viable count assays were the cancer cells on the chart that had below the 50% benchmark. Relative standard deviation of 5.0% (n=4). The table for the analysis follows in Table 1.

## 4. SNP:PEG : KPFE composite scaffold assays

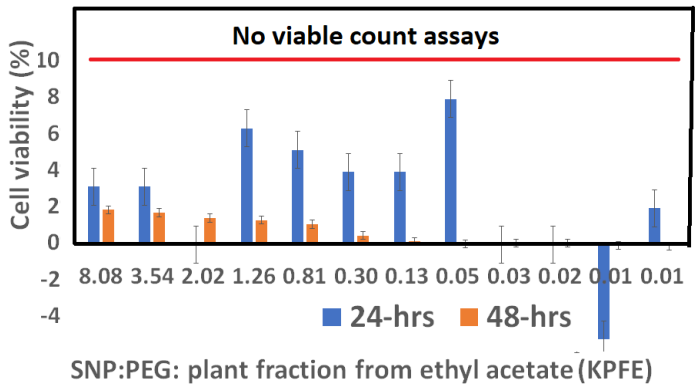


## 5. SNP : PEG : KPLM composite scaffold assays

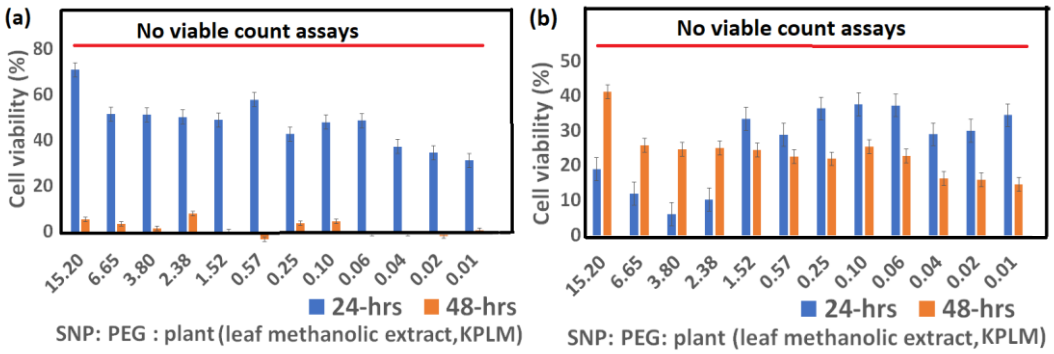


**Fig.3.** Cancer cell viability of SNP/plant extracts derived scaffolds. Breast cancer cells of MCF-7 were exposed to synthetic derived materials. The substrate casts were developed under: (a) low humidity conditions (b) high humidity conditions as described in the methods section. The horizontal line above the bar charts indicate counting systems used to differentiate the viable count assays from the no viable count assays. Additionally, the data on the horizontal axis of charts : 4 and 5, represent the concentration ratios that have been simplified (actual concentrations were used for the inhibitory concentrations of figure plots 4 and 5 in Figure 5). The assay was considered viable when the viability of cancer cells was at least above 50%. Additionally, the 50% cell viability above benchmark were the cancer cells unaffected to scaffold exposure after 48 hrs. No viable count assays were the cancer cells on the chart that had below the 50% benchmark. Relative standard deviation of 5.0% (n=4). The table for the analysis follows in Table 1.

**Table 1.** MCF-7 cells profiling exposed to different scaffold-composite assays

| **(Substrate cast type) Material components of scaffold fabrication** | **Scaffold fabricated from a low humidity chamber** | | **Scaffold fabricated from a high humidity chamber** | |
|---|---|---|---|---|
| | **Total assay count* (%)** | ***p*-value**** | **Total assay* count (%)** | ***p*-value**** |
| 1. SNP | 67 | 0.11 | 83 | 0.09 |
| 2. SNP : PEG | 0 | 0.004 | 0 | 0.003 |
| 3. SNP: PEG : Dendrimer | 83 | 0.36 | 0 | 0.64 |

| | | | | |
|---|---|---|---|---|
| 4. SNP: PEG : KPFE | 0 | 0.004 | nd | n/a |
| 5. SNP: PEG : KPLM | 0 | 0.13 | 0 | 0.001 |

* The total assay count was calculated as the : $Total\ count\ of\ viable\ assays / Total\ assays$ .The total assay represents the number of assays (N=12). The viable count assays were the cancer cells that were unaffected to scaffold exposure after 48 hrs.

**$p$-value represents the statistical relevance of data. The data relevance was considered using the confidence interval limit of $0 < p < 0.06$

nd Not determined

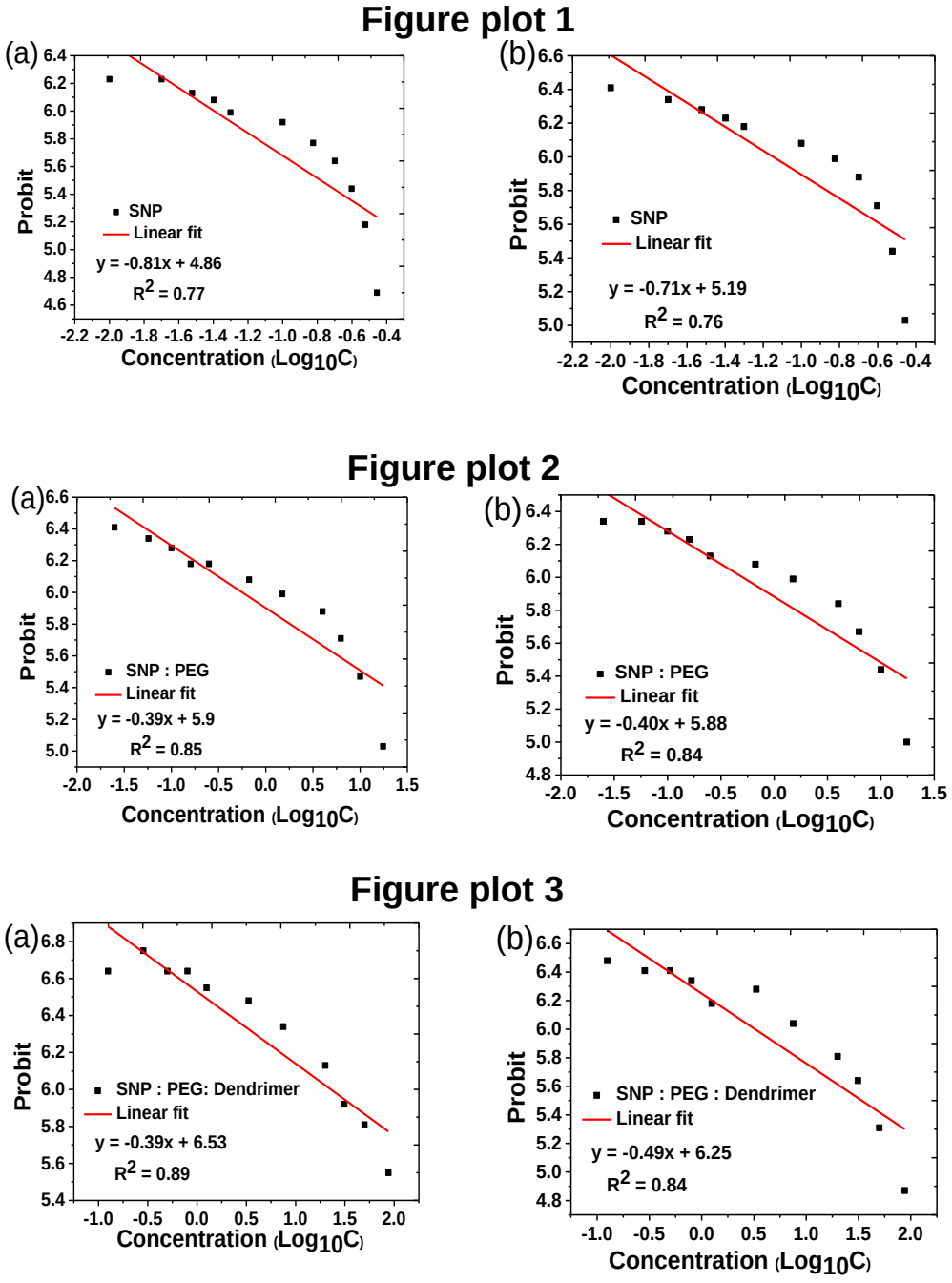


**Fig. 4.** Inhibitory concentration ($IC_{50}$) plots of cancer cells exposed to scaffold assays that were based on synthetic materials developed under (a) low humidity conditions (b) high humidity conditions. Figure plots: (1) SNP (2) SNP : PEG (3) SNP:PEG: dendrimer. The $IC_{50}$ is the inhibitory scaffold concentration that potentially contributes to the inhibition of cancer cells after 48 hrs. The probit

represents the transformation of the cell viability (%). This transformation was carried out using the probit analysis table. The logarithmic concentration represented on the x-axis is the concentration ratio of the composite mixture. $R^2$, shows the regression of the line fitting, suggesting the $IC_{50}$ used here is only indicating a projected inhibition concentration. The table for the analysis follows in Table 2.

**Figure plot 4**

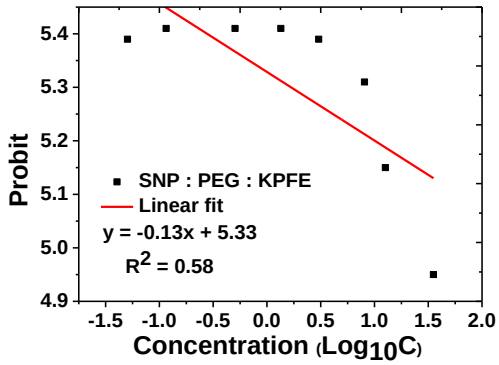


**Figure plot 5**

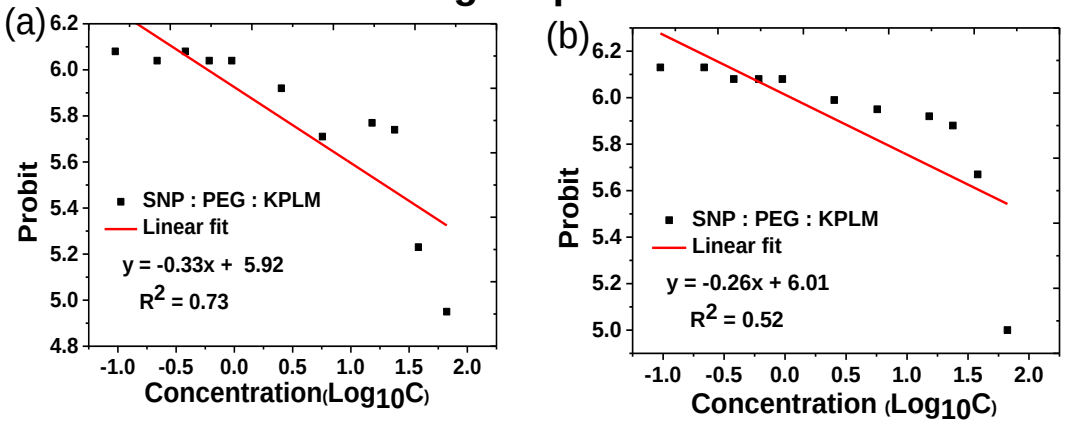


**Fig. 5.** Inhibitory concentration ($IC_{50}$) plots of cancer cells exposed to scaffold assays that were based on synthetic materials/plant extracts developed under (a) low humidity conditions (b) high humidity conditions. Figure plots: (4) SNP: PEG: KPFE; (5) SNP:PEG: KPLM. The $IC_{50}$ is the inhibitory scaffold concentration that potentially contributes to the inhibition of cancer cells after 48 hrs. The probit represents the transformation of the cell viability (%). This transformation can easily be carried out using the probit analysis table. The logarithmic concentration represented on the x-axis is the concentration ratio of the composite mixture. $R^2$, shows the regression of the line fitting, suggesting the $IC_{50}$ used here is only indicating a projected inhibition concentration. The table for the analysis follows in Table 2.

**Table 2.** Assessment of the therapeutic safety of cancer cells exposed to scaffold assays

| Components | Calculated ($IC_{50}$) for scaffold developed using a low humidity chamber | Calculated ( $IC_{50}$) for scaffold developed using a high humidity chamber |
|---|---|---|
| 1. SNP | > 0.18 wt.% | > 0.18 wt.% |
| 2. SNP:PEG | > 2.9 (ratio) | > 3.3 (ratio) |
| 3. SNP: PEG: Dendrimer | > 10 mg/mL | > 15.8 mg/mL |
| 4. SNP: PEG: KPFE | > 14. 1 mg/mL | nd |
| 5. SNP: PEG: KPLM | > 17.4 mg/mL | >50 mg/mL |

nd = Not determined

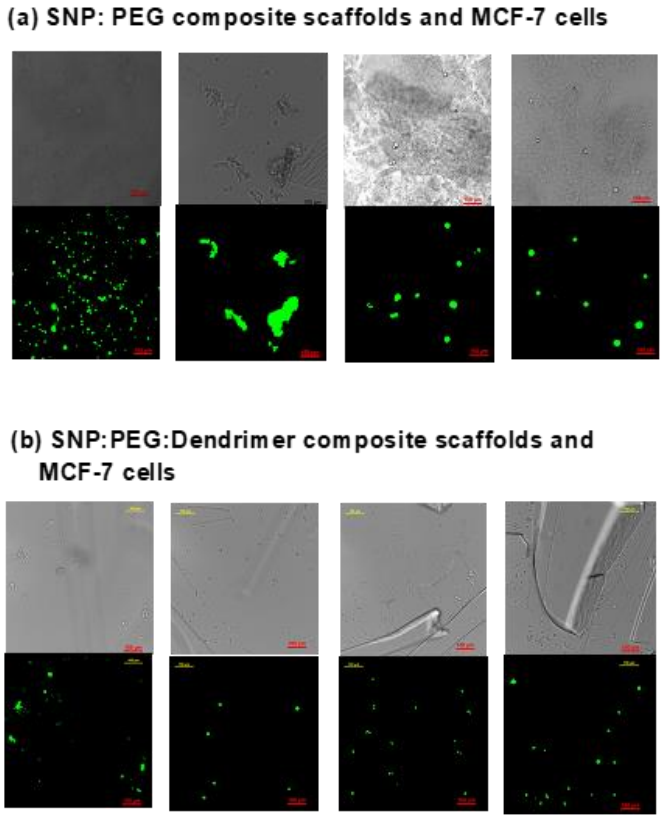


**Fig. 6.** Bright field/fluorescence imaging. Cell viability of MCF-7 cells exposed to synthetic materials for 24 hrs. From left to right : (a) 2- composite substrate. The SNP: PEG ratio respectively: 40:1, 20:5, 5:20 and 3:30 (b) 3-composite substrate. The SNP : PEG: Dendrimer ratio respectively: 40:1:20, 20:5:20, 5:20:20 and 3:30:20. The concentration of cells plated on the substrate cast was for 24 hrs at $10^3$ cells $mL^{-1}$. The green, fluorescent dye (cytopainter) was used to track live cancer cells. The fluorescent cells are enhanced upon entering the cells. The green dye was visualized under the fluorescence microscope using a green filter (Ex/Em = 490/520 nm) within 24 hrs (scale bar = 100 µm). Based on the total assay count in Table 1, substrate cast exhibits (a): inhibition cell-based assay (b) proliferating assay.

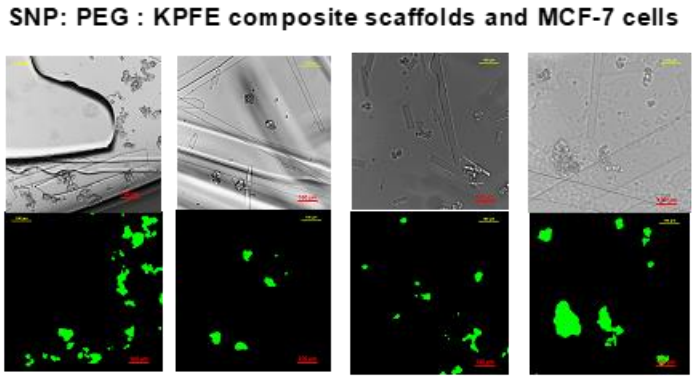


**Fig. 7.** Bright field/fluorescence imaging. Cell viability of MCF-7 cells exposed to synthetic/plant extracts for 24 hrs.The formulation mixture of SNP:PEG was varied and KPFE concentration remained the same before solvent was evaporated, according to the mixture ratio : 81, 20, 8, 1. (scale bar = 100 µm). The concentration of cells plated on the substrate cast was for 24 hrs at $10^3$ cells $mL^{-1}$ produce clustered cells that are only short-lived. The green, fluorescent dye (cytopainter) was used to track live cancer cells. The fluorescent cells are enhanced upon entering the cells. The green dye was visualized under the fluorescence microscope using a green filter (Ex/Em = 490/520 nm) within 24 hrs. Again, based on the total assay count in Table 1, the substrate cast in each panel exhibits inhibition cell-based assay.

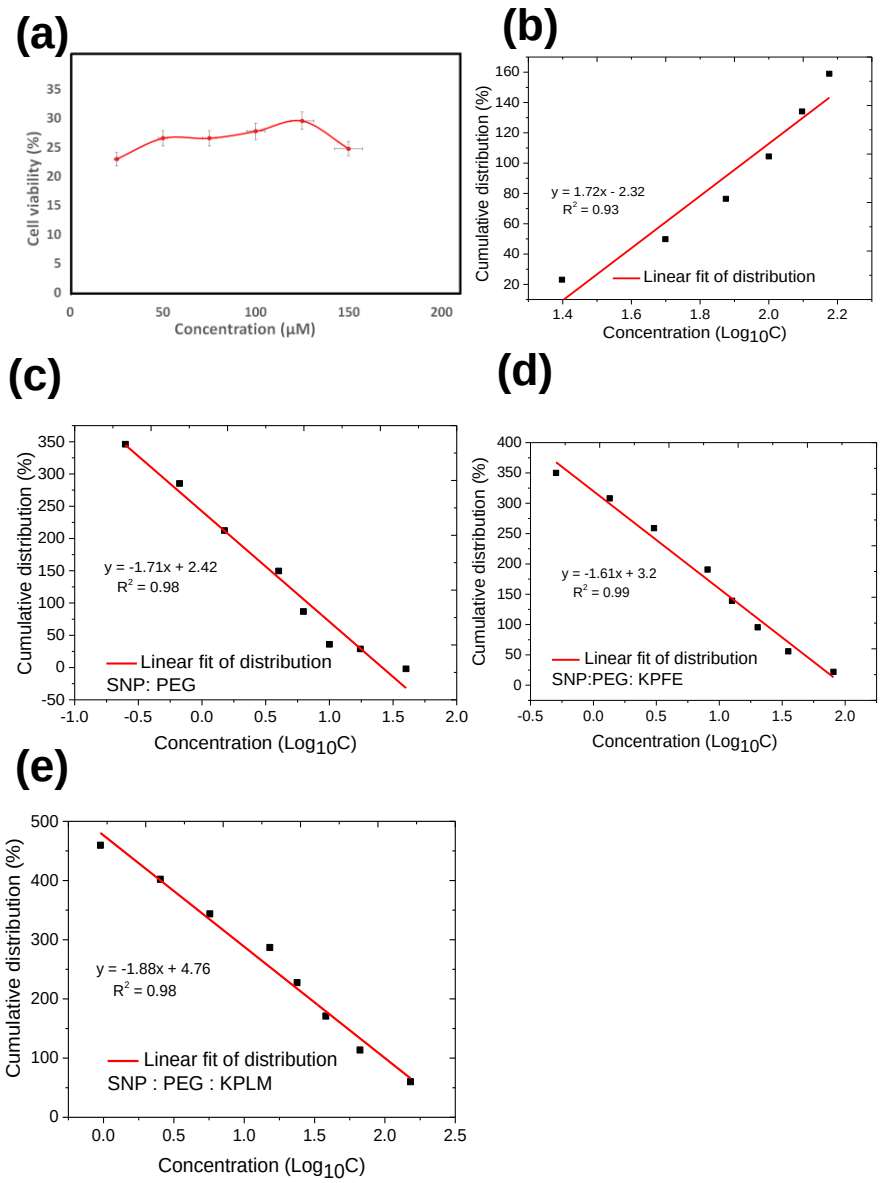


**Fig. 8.** Cisplatin dosing on carcinoma of MCF-7 breast cancer cells grown in a standard 96-well plate. (a) Cancer cell viability responses at varying cisplatin dosing. Relative standard deviation of 5.0% (n=4) .The cumulative distribution plot was used to calculate the inhibitory dosing effect that reduced the cell viability by at least 50% (b) directly in a 96 well plate. Composite scaffolds of : (c) SNP: PEG (d) SNP : PEG : KPFE (e) SNP: PEG : KPLM. The cumulative distribution was obtained by adding the successive cell viability (%) values. Subsequently, the 50% of the cumulative distribution was used for the calculation of the $IC_{50}$. The cancer cells were plated at 10,000 cells using 100 µL volume, with 200 µL of cisplatin concentration added to each test samples.

**Table 3**. Cisplatin dosing concentration that reduced the cell viability by at least 50%

| **Components** | **Combined cisplatin dosing /scaffold (μM)** |
|---|---|
| 1. Control plate (without scaffold) | 64 |
| 2. SNP:PEG | 2.5 |
| 3. SNP: PEG: KPFE | 80 |
| 4. SNP: PEG: KPLM | 20 |

Abbreviations used
MCF-7 = Breast cancer cell line
SNP = Silica nanoparticles
MTS = [3-(4,5-dimethylthiazol-2-yl)-5-(3-carboxymethoxyphenyl)-2-(4-sulfophenyl)-2H-tetrazolium]
ECM = Extracellular matrix
PEG = Polyethylene glycol
PEGylated SNP = Composite scaffolds derived from SNP : PEG formulation mixtures
1º PAMAM = Polyamidoamine first generation
DMEM = Dulbecco's Modified Eagle Medium
FBS = fetal bovine serum
HBSS = Hanks balanced salt solution
SEM = Scanning electron microscopy
PVC = Polyvinyl chloride
*T. ferdinandiana* = *Terminalia ferdinandiana* Exell
KPLM = *T. ferdinandiana* leaf methanolic extract
KPFE = *T. ferdinandiana* fruit ethyl acetate extract
$IC_{50}$ = Inhibitory concentration (Scaffold inhibition concentration to cancer cells)

# Profiling the neoplasm microenvironment of silica nanomaterial-derived scaffolds of single, 2- and 3-composite systems

Victor Akpe[1, 2*], Shweta Murhekar[1, 2], Tak H. Kim[1, 2], Christopher L. Brown[1, 2] and Ian E. Cock[1, 2*]

[1] School of Environment and Science, Griffith University, Nathan Campus, QLD 4111, Australia.

[2] Environmental Futures Research Institute, Griffith University, Nathan Campus, QLD 4111, Australia.

*Correspondence: I.Cock@griffith.edu.au

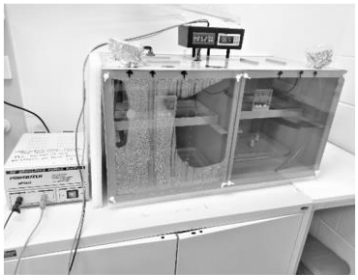

**Fig. S1.** Digital image. Fabrication chamber used to develop substrate cast under low and high humidity conditions. Chamber specifications: (Δ = 37 °C, 15% humidity and 30 °C, 90% humidity) with ± 3 % humidity and temperature fluctuations. The chamber consists of polyvinyl chloride (PVC) rectangular box, Peltier heaters, heating pads, (RadioShack) attached to 12V DC Micro Fan and two humidity-temperature monitors. The moisture content in both chambers was adjusted by, (1) filling one of the lower chamber trays with water (2) Perforating the upper shelves in both boxes to create sufficient convective airflow. The chamber was used to fabricate the substrate cast only. The standard incubator chamber was used for the incubation of cancer cells seeded on the scaffolds.

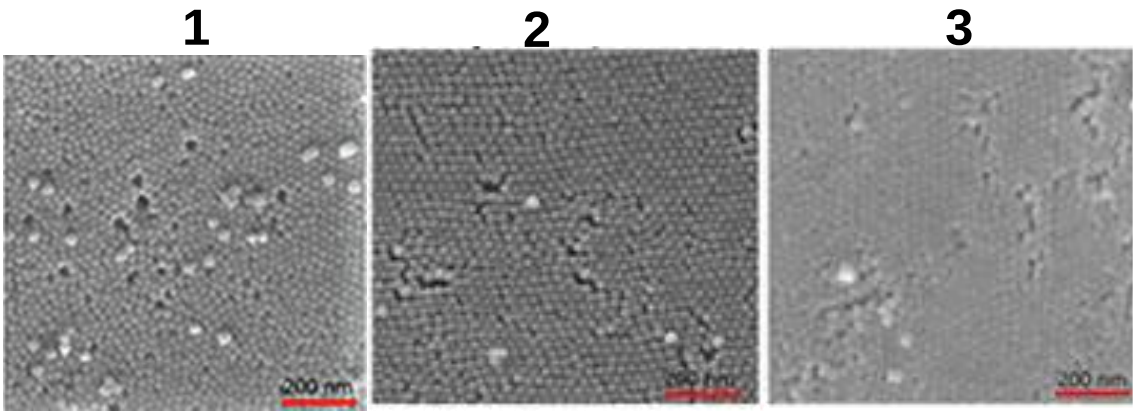


**Fig. S2.** SEM micrographs. The images indicate the tightly packed configurations of : (1) SNP (2) SNP: PEG, and (3) SNP : PEG : Dendrimer are driven by van der Waals and other short-range intermolecular forces at the nano level. These configurations are not rigid but temporary. These micrographs were substrate casts fabricated under low humidity conditions using the fabrication chamber in Fig. S1. (scale bar = 200 nm).

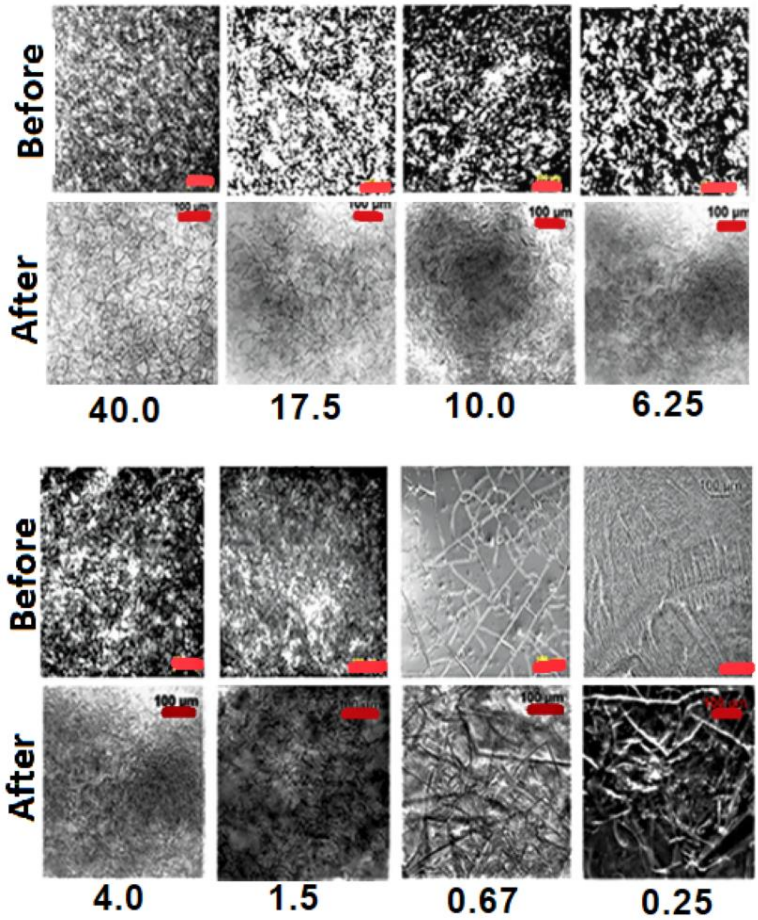


**Fig. S3**. Scaffold composites of SNP:PEG mixtures produced under high humidity conditions. The bright field images indicate that the landscape changed after exposure to MCF-7 cells. These images were taken after 12 hours of seeding the cancer cells on the substrate casts. The SNP : PEG formulation ratio (SNP to PEG): 40 .0 , 17.5 , 10.0 , 6.25 , 4.0 ,1.5 , 0.67, and 0.25. The concentration of cells plated on the substrate cast was for 24 hrs at $10^3$ cells $mL^{-1}$. (scale bar = 100 µm).

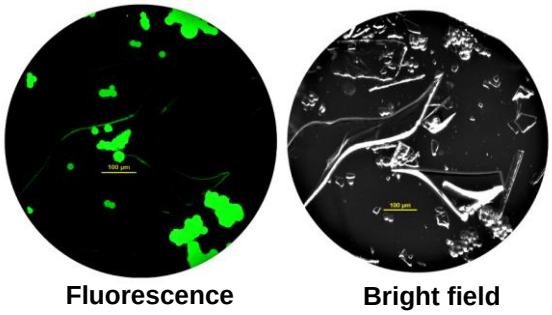


**Fig. S4**. Scaffold composites of SNP: PEG mixtures with landscape changes. These images were taken after 24 hours exposure of MCF-7 cells. The concentration of cells plated on the substrate cast was for 24 hrs at $10^3$ cells $mL^{-1}$. The green, fluorescent dye (cytopainter) was used to track live cancer cells. The fluorescent cells are enhanced upon entering the cells. The green dye was visualized under the fluorescence microscope using a green filter (Excitation/Emission = 490/520 nm) within 24 hrs. (scale bar = 100 µm).

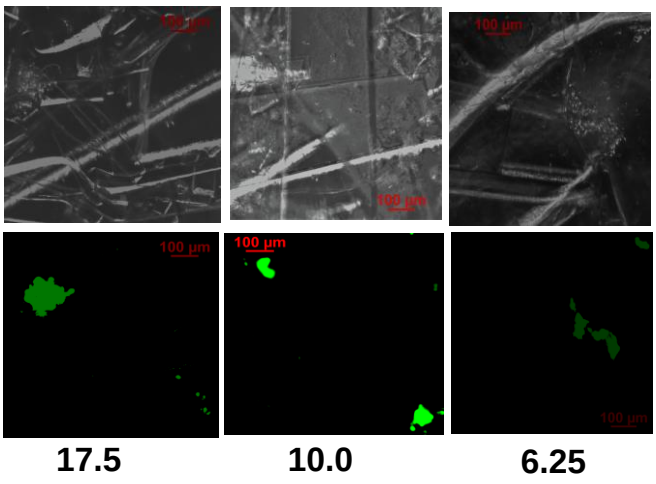


**Fig.S5.** Scaffold composites of SNP: PEG mixtures with landscape changes. These images were taken after 48 hours exposure of MCF-7 cells. The numbers displayed represent the SNP: PEG formulation ratio used to prepare the scaffold. The concentration of cells plated on the substrate cast was for 24 hrs at $10^3$ cells $mL^{-1}$. The green, fluorescent dye (cytopainter) was used to track live cancer cells. The fluorescent cells are enhanced upon entering the cells. The green dye was visualized under the fluorescence microscope using a green filter (Excitation/Emission = 490/520 nm) within 48 hrs. (scale bar = 100 µm).

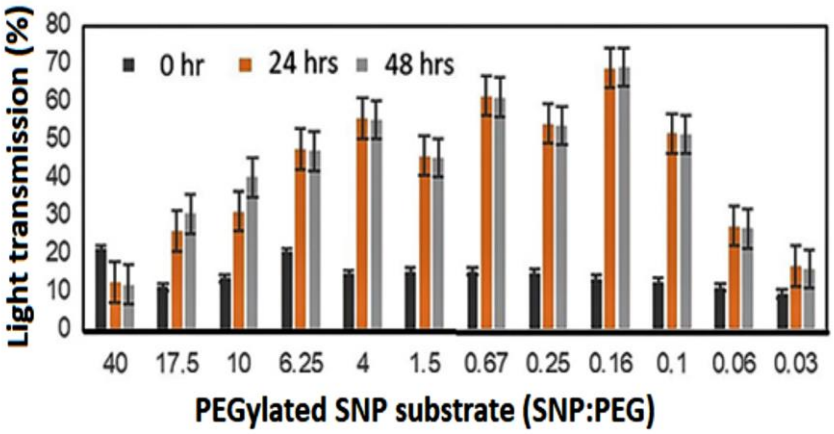


**Fig.S6.** Effect of light transmission on substrate cast (SNP : PEG) at different intervals. Here, the substrate cast was exposed to UV light at the excitation wavelength (490nm) with the UV-plate reader. The 0-hr (black bar) indicate the recorded readings after the substrate cast was fabricated. The 24 hrs (brown bar) were the recorded readings after the substrate casts were incubated using the standard cell culture chamber. The 48-hr(grey bar) were the recorded readings after the substrate casts were incubated using the standard cell culture chamber. The SNP: PEG mixtures were cast into the 96-well plate using the customized chamber, under the low humidity conditions. The substrates were dried before the measurements were recorded using a plate reader. Relative standard deviation of 5.0% (n=4)

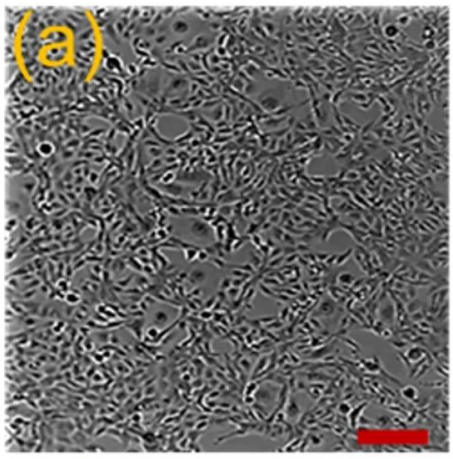


**Fig.S7. (a)** MCF-7 cells cultured using the standard culture flask. The cells show a flat, extended network on the culture flask(scale bar=100 µm).

# Tables

Table S1. Preparation of single, 2- and 3- composite mixtures. Z= PAMAM ($1^{O}$) Dendrimer (20 wt.% dissolved in methanol)

| SNP (X) (wt.%) | V(mL) | $V_{water}$(mL) | PEG (Y) (wt.%) | X: Y | X:Y: Z |
|---|---|---|---|---|---|
| 40 | 10.00 | 0.00 | 1 | 40.1 | 40:1:20 |
| 35 | 8.75 | 1.25 | 2 | 35:2 | 35:2:20 |
| 30 | 7.50 | 2.50 | 3 | 30:3 | 30:3:20 |
| 25 | 6.25 | 3.75 | 4 | 25:4 | 25:4:20 |
| 20 | 5.00 | 5.00 | 5 | 20:5 | 20:5:20 |

| | | | | | |
|---|---|---|---|---|---|
| 15 | 3.75 | 6.25 | 10 | 15:10 | 15:10:20 |
| 10 | 2.50 | 7.50 | 15 | 10:15 | 10:15:20 |
| 5 | 1.25 | 8.75 | 20 | 5:20 | 5:20:20 |
| 4 | 1.00 | 9.00 | 25 | 4:25 | 4:25:20 |
| 3 | 0.75 | 9.25 | 30 | 3:30 | 3:30:20 |
| 2 | 0.50 | 9.50 | 35 | 2:35 | 2:35:20 |
| 1 | 0.25 | 9.75 | 40 | 1:40 | 1:40:20 |

A semi-qualitative data is in Tables S2 to S4 for the cell viability (%) at 24- and 48 hrs. The cellular viability scores ≤ 50 % on test samples are considered as non-viable and scores > 50 % as viable cells, according to this paper.[1]

Table S2. Viability test for a single component substrate.

| | | Low humidity | | High humidity | |
|---|---|---|---|---|---|
| **Well** | **Conc. (wt.%)** | **24 hrs** | **48 hrs** | **24 hrs** | **48 hrs** |
| 1 | 40 | Non-viable | Non-viable | Viable | Non-viable |
| 2 | 35 | Viable | Non-viable | Viable | Viable |
| 3 | 30 | Viable | Non-viable | Viable | Viable |
| 4 | 25 | Viable | Viable | Viable | Viable |
| 5 | 20 | Viable | Viable | Viable | Viable |
| 6 | 15 | Viable | Viable | Viable | Viable |
| 7 | 10 | Viable | Viable | Viable | Viable |
| 8 | 5 | Viable | Viable | Viable | Viable |
| 9 | 4 | Viable | Viable | Viable | Viable |
| 10 | 3 | Viable | Viable | Viable | Viable |
| 11 | 2 | Viable | Viable | Viable | Viable |
| 12 | 1 | Viable | Non-viable | Viable | Non-viable |

Table S3. Viability test for a 2-composite substrate.

| | | Low humidity | | High humidity | |
|---|---|---|---|---|---|
| **Well** | **Conc.** | **24 hrs** | **48 hrs** | **24 hrs** | **48 hrs** |
| 1 | 40: 1 | Viable | Non-viable | Non-viable | Non-viable |
| 2 | 35:2 | Viable | Non-viable | Viable | Non-viable |
| 3 | 30:3 | Viable | Non-viable | Viable | Non-viable |
| 4 | 25:4 | Viable | Non-viable | Viable | Non-viable |
| 5 | 20:5 | Viable | Non-viable | Viable | Non-viable |

| | | | | | |
|---|---|---|---|---|---|
| 6 | 15:10 | Viable | Non-viable | Viable | Non-viable |
| 7 | 10:15 | Viable | Non-viable | Viable | Non-viable |
| 8 | 5:20 | Viable | Non-viable | Non-viable | Non-viable |
| 9 | 4:25 | Viable | Non-viable | Non-viable | Non-viable |
| 10 | 3:30 | Non-viable | Non-viable | Non-viable | Non-viable |
| 11 | 2:35 | Non-viable | Non-viable | Non-viable | Non-viable |
| 12 | 1:40 | Non-viable | Non-viable | Non-viable | Non-viable |

Table S4. Viability test for a 3-composite substrate.

| | | **Low humidity** | | **High humidity** | |
|---|---|---|---|---|---|
| | | | | | |
| **Well** | **Conc.** | **24 hrs** | **48 hrs** | **24 hrs** | **48 hrs** |
| 1 | 40:1:20 | Non-viable | Viable | Non-viable | Non-viable |
| 2 | 35:2:20 | Non-viable | Viable | Viable | Non-viable |
| 3 | 30:3:20 | Non-viable | Non-viable | Non-viable | Non-viable |
| 4 | 25:4:20 | Non-viable | Viable | Non-viable | Non-viable |
| 5 | 20:5:20 | Non-viable | Viable | Non-viable | Non-viable |
| 6 | 15:10:20 | Non-viable | Viable | Non-viable | Non-viable |
| 7 | 10:15:20 | Non-viable | Viable | Non-viable | Non-viable |
| 8 | 5:20:20 | Non-viable | Viable | Non-viable | Non-viable |
| 9 | 4:25:20 | Non-viable | Viable | Non-viable | Non-viable |
| 10 | 3:30:20 | Non-viable | Viable | Non-viable | Non-viable |
| 11 | 2:35:20 | Non-viable | Viable | Non-viable | Non-viable |
| 12 | 1:40:20 | Non-viable | Non-viable | Viable | Non-viable |

# Supplementary reference

**S**1. Shalom J, Cock IE: Terminalia ferdinandiana Exell. fruit and leaf extracts inhibit proliferation and induce apoptosis in selected human cancer cell lines. *Nutrition and Cancer* 2018; **70**, 579-593.